X-Ray Absorption Near-Edge Structure (XANES) Spectroscopy Study of the Interaction of Silver Ions with *Staphylococcus aureus*, *Listeria monocytogenes*, and *Escherichia coli*

Gudrun Lisa Bovenkamp,[a,b] Ulrike Zanzen,[c] Katla Sai Krishna,[b] Josef Hormes,[a,b,d] Alexander Prange[b,c,e]

Institute of Physics, University of Bonn, Bonn, Germany[a]; Center for Advanced Microstructures and Devices (CAMD), Louisiana State University, Baton Rouge, Louisiana, USA[b]; Competence Center for Microbiology & Biotechnology (CCMB), Niederrhein University of Applied Sciences, Mönchengladbach, Germany[c]; Canadian Light Source (CLS), University of Saskatchewan, Saskatoon, Saskatchewan, Canada[d]; Institute for Virology and Microbiology, University of Witten/Herdecke, Witten, Germany[e]

Silver ions are widely used as antibacterial agents, but the basic molecular mechanism of this effect is still poorly understood. X-ray absorption near-edge structure (XANES) spectroscopy at the Ag *LIII*, S *K*, and P *K* edges reveals the chemical forms of silver in *Staphylococcus aureus* and *Escherichia coli* (Ag$^+$ treated). The Ag *LIII*-edge XANES spectra of the bacteria are all slightly different and very different from the spectra of silver ions (silver nitrate and silver acetate), which confirms that a reaction occurs. Death or inactivation of bacteria was observed by plate counting and light microscopy. Silver bonding to sulfhydryl groups (Ag-S) in cysteine and Ag-N or Ag-O bonding in histidine, alanine, and DL-aspartic acid was detected by using synthesized silver-amino acids. Significantly lower silver-cysteine content, coupled with higher silver-histidine content, in Gram-positive *S. aureus* and *Listeria monocytogenes* cells indicates that the peptidoglycan multilayer could be buffering the biocidal effect of silver on Gram-positive bacteria, at least in part. Bonding of silver to phosphate groups was not detected. Interaction with DNA or proteins can occur through Ag-N bonding. The formation of silver-cysteine can be confirmed for both bacterial cell types, which supports the hypothesis that enzyme-catalyzed reactions and the electron transport chain within the cell are disrupted.

Silver has been used as an inorganic antibacterial agent for centuries. Its antimicrobial effects are currently used in a variety of biological, medical, and hygienic applications, for example, as an antifungal agent, in antibacterial agents for antibiotic-resistant bacteria, in silver-based antiseptics, etc. (1–4). Silver ions (Ag$^+$) and several compounds containing silver ions are highly toxic to microorganisms and exhibit strong biocidal effects on many species of bacteria. Their toxicity to bacterial cells varies widely among bacteria. Kim and coworkers, for example, reported that low concentrations of silver nanoparticles strongly inhibit the growth of *Escherichia coli*, whereas the growth-inhibitory effects on *Staphylococcus aureus* are mild (5). Some bacteria even exhibit complete resistance to silver, as seen in *E. coli* mutants displaying active efflux of silver ions (6) and efflux-mediated heavy metal resistance in general (7). Reducing the particle size of the corresponding materials, i.e., using silver nanoparticles instead of bulk silver, yields increased antibacterial activity (5). Although silver ions (e.g., silver nitrate) and silver nanoparticles are already widely used for various antibacterial purposes, the exact antibacterial mechanism has not yet been elucidated. Within the last 30 years, quite a number of attempts have been made to interpret the antimicrobial mechanism of silver ions and silver nanoparticles. These hypotheses can be summarized as (i) bonding of Ag to amino acids in proteins and enzymes, especially via sulfur or via nitrogen; (ii) bonding to nucleic acids and phosphates in DNA or RNA; and (iii) oxidation catalyzed by Ag. These bonding reactions can cause, e.g., structural changes in the cell wall and bacterial membrane, disruption of enzyme-catalyzed reactions, or disruption of the electron transport chain of the cell (8–11). On the basis of chemical and microbiological experiments with *Pseudomonas aeruginosa*, it has been proposed that the mechanism of the antibacterial activity of silver closely correlated with the interactions of silver with thiol (S-H) groups (12), although other targets, such

as amine (N-H) groups, have also been discussed (3, 13, 14). In their experiments observing the growth inhibition of silver compounds containing thiol groups versus silver compounds not containing thiol groups, it was found (5, 12) that compounds containing thiol groups (e.g., in cysteine) neutralize the antibacterial activity of silver completely; i.e., these compounds do not show any antibacterial effect. L-Cystine dimethyl ester (not containing thiol groups) did not neutralize the antibacterial activity of silver (12). Together with the observation that silver bonding to sulfur is stronger than silver bonding to nitrogen (9), these examples indicate that silver prefers sulfur bonding only when delivered by non-sulfur-containing agents; in such cases, silver compounds can become effective antibacterial agents. Besides biochemical or physiological experiments, morphological data on cell disruption caused by silver ions were published (3). However, in all of the studies performed so far, direct experimental evidence is lacking on a molecular level for the binding of silver in bacteria and potential differences in the chemical environment of the silver ions interacting with various microorganisms. To analyze the molecular reactions of silver ions, an *in situ* tool for analysis of the chemical forms of silver on an atomic or molecular level such as X-ray absorption near-edge structure (XANES) spectroscopy is the method of choice to address these open questions. XANES allows not only the determination of the valence of an excited atom but

TABLE 1 LCF results for silver *LIII*-edge XANES spectra of silver ion-treated bacteria with silver reference compounds silver-cysteine, silver-histidine, silver-alanine, and silver–DL-aspartic acid

Sample	% contributions to different chemical forms of silver[a]			
	Silver-cysteine	Silver-histidine	Silver-alanine	Silver–DL-aspartic acid
E. coli + silver nitrate	24	10	37	29
S. aureus + silver nitrate	10	47	40	3
L. monocytogenes + silver nitrate	14	47	26	13

[a] The percentage contributions of different silver species to the chemical forms of silver are shown; there was less than $\pm 10\%$ error.

also gives information about the type of neighboring atoms (15). This information about the actual binding of silver can often be deduced by comparing the XANES spectrum of the sample of interest with the spectra of suitable model (reference) compounds ("fingerprint" analysis). This technique using synchrotron radiation is generally a powerful tool to probe the chemical forms of an element in complex (biological) materials, e.g., determination of the chemical forms of sulfur in biological samples (16–19), determination of the chemical forms of silver in silver silicate gels (20), or determination of the chemical forms of phosphorus in soils (21). Various Ag *L*-edge XANES spectra of silver oxides have been reported by Behrens et al. (22). They show that the oxidation state is reflected in the XANES spectra. The key advantages are that XANES spectroscopy is nondestructive and that measurement can be performed *in situ* (e.g., aquatic environmental samples and cultured bacteria in liquid media) (23 and references therein). It was the aim of this study to analyze the basic mechanism of silver ions as antibacterial agents and to investigate the "most likely elemental bonding partners" of silver ions through the application of XANES spectroscopy at the silver *LIII* edge, sulfur *K* edge, and phosphorus *K* edge on bacteria treated with silver ions. These XANES spectra should give information about the interaction of silver ions with cells and about the determination of the chemical forms of silver that are present after the reaction.

Two questions were the focus in this study, i.e., (i) what is the preferred bonding target of the silver ion when reacting with bacteria and (ii) which of the hypotheses regarding the reactions of silver discussed in the literature can be corroborated or ruled out? The human-pathogenic Gram-positive bacteria *S. aureus* and *Listeria monocytogenes* and Gram-negative *E. coli* were chosen as model organisms because they have been widely used as test organisms in other investigations related to the antibacterial activity of silver ions or silver nanoparticles (23). Furthermore, Gram staining characteristics, i.e., the peptidoglycan multilayer, may have an effect on the interaction of silver ions.

MATERIALS AND METHODS

Bacterial strains, media, cultivation, and sample preparation. *S. aureus* DSMZ 2569, *E. coli* DSMZ 1103, and *L. monocytogenes* DSMZ 20600 were grown in a shaker for 24 to 48 h at 30°C in yeast-peptone-dextrose broth

(10 g yeast extract, 20 g peptone, and 20 g dextrose [YPD broth from Difco Becton Dickinson, Franklin Lakes, NJ] without sodium chloride). Bacteria were washed and centrifuged twice. The bacteria were diluted to 10^6 CFU/ml with sterile deionized water (to avoid chemical reactions of silver ions with medium contents), and then 50 μl of a 0.1 M silver nitrate stock solution or 50 μl of a 0.1 M silver acetate stock solution, respectively (both powders from Sigma-Aldrich, St. Louis, MO), was added to 1 ml cell culture (about to 10^6 CFU/ml). The samples were incubated at 20°C for 10 min in darkness and then washed again with 0.5 ml water to remove unreacted silver compounds. About 20 μl cell material was put on filter paper and attached to Kapton tape. These samples were dried in darkness for 1 to 2 h. A control set was prepared as described above without adding Ag-containing solutions. Samples for XANES analysis were prepared and handled according to Prange et al. (18).

Experimental XANES spectroscopy. Silver *LIII* edge, sulfur *K* edge, and phosphorus *K*-edge XANES spectra were recorded at the double-crystal monochromator (DCM) beamline of the Center for Advanced Microstructures and Devices (CAMD), Louisiana State University, Baton Rouge, LA (24). The monochromator was equipped with InSb(111) crystals. Measurements of the bacterial samples at the silver *LIII* edge, sulfur *K* edge, and phosphorus *K* edge were performed in fluorescence mode with a Vortex silicon drift detector (SII Nano Technology Inc.) to record the fluorescence photons and an ionization chamber for the incident photons with 90 mbar nitrogen pressure at the Ag *LIII* edge, 60 mbar nitrogen pressure at the S *K* edge, and 27 mbar nitrogen pressure at the P *K* edge inside the ionization chambers and sample chambers. For energy calibration of the silver spectra, the spectrum of elemental silver (made from silver flake powder) was used as a "secondary standard," setting the maximum of the first peak in the derivative of the spectrum to an energy of 3,351 eV. According to the minimum step width, the energy value is reproducible within ± 0.2 eV. Silver spectra were scanned with step widths of 1 eV in the pre-edge region between 3,300 and 3,330 eV; 0.2 eV between 3,330 and 3,400 eV, the main region of interest; and 0.5 eV between 3,400 and 3,500 eV with an integration time of 1 s per point. Measurements of the silver reference compounds (see Fig. 2) were performed with the same step sizes and parameters in transmission mode. For the synthesis of silver-amino acids, high-purity L-histidine, DL-aspartic acid, L-alanine, and L-cysteine were purchased from Sigma-Aldrich. Ag-histidine was prepared by the method reported by Nomiya et al. (25). Ag–DL-aspartic acid was prepared by the method reported by Nomiya and Yokoyama (26). Ag-cysteine was prepared by the method reported by Pakhomov et al. (27). Ag-alanine was prepared by the method reported by Demaret and Abraham (28). X-ray diffraction and Fourier transform infrared spectros-

TABLE 2 LCF results for sulfur *K*-edge XANES spectra of silver ion-treated bacteria with sulfur reference compounds silver-cysteine, silver-glutathione, L-cysteine, L-glutathione, methionine, and zinc sulfate

Sample	% contribution to different chemical forms of silver[a]					
	Silver-cysteine	Silver-glutathione	L-Cysteine	L-Glutathione	Methionine	Zinc sulfate
E. coli + silver nitrate	63	—	—	37	—	—
S. aureus + silver nitrate	63	—	—	37	—	—

[a] The percentage contributions of different sulfur species to the chemical forms of sulfur are shown; there was less than $\pm 10\%$ error. —, contribution of <3%.
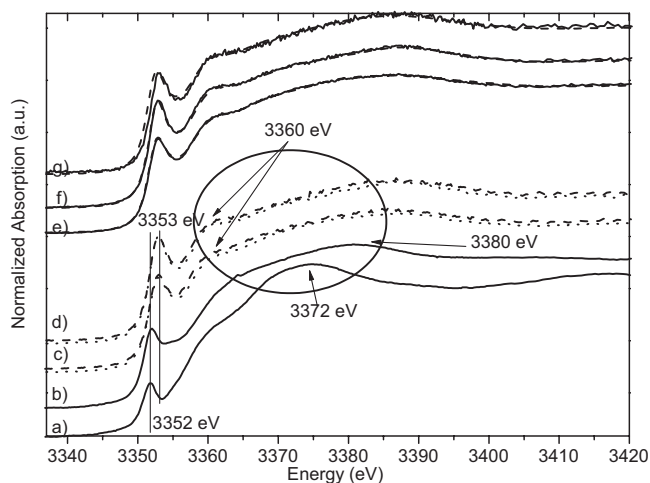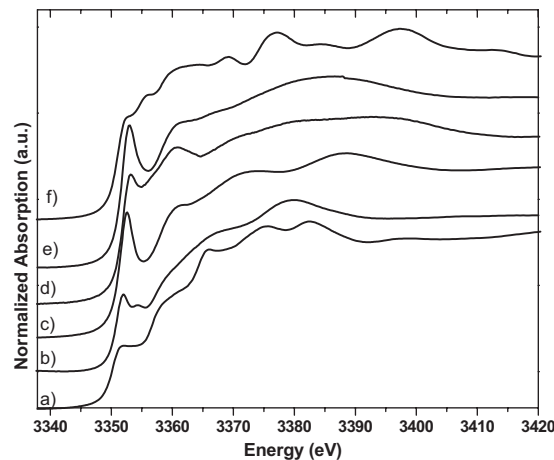
FIG 1 Silver *LIII*-edge XANES spectra of silver nitrate solution (solid line) (a), silver acetate solution (solid line) (b), *E. coli* cells treated with silver nitrate (dotted line) or silver acetate (broken line) (c), *S. aureus* cells treated with silver nitrate (dotted line), and *S. aureus* cells treated with silver acetate (broken line) (d); LCF of *E. coli* cells treated with silver nitrate according to Table 1 (broken line) and the experimental results (solid line) (e); LCF of *S. aureus* cells treated with silver nitrate according to Table 1 (broken line) and the experimental results (solid line) (f); and LCF of *L. monocytogenes* cells treated with silver nitrate according to Table 1 (broken line) and the experimental results (solid line) (g). a.u., arbitrary units.

FIG 2 Silver *LIII*-edge XANES spectra of silver reference compounds silver phosphate (a), silver–DL-aspartic acid (b), silver-alanine (c), silver-cysteine (d), silver-histidine (e), and silver metal (f). a.u., arbitrary units.

copy confirmed the reported structures. Data were normalized and analyzed with the ATHENA program of the IFFEFIT package (29). The error of the percentage contributions for the compounds in the linear combination fitting (LCF) results (Tables 1 and 2) can be estimated to $\pm 10\%$ (according to reference 18).

For energy calibration of the sulfur and phosphorus spectra, the spectrum of zinc sulfate was used as a "secondary standard," setting the maximum of the white line of the sulfur *K*-edge spectrum to an energy of 2,481.4 eV. According to the minimum step width, the energy value at both edges is reproducible within ± 0.1 eV. Bacterial sulfur (phosphorus in parentheses) spectra were scanned with step widths of 0.5 eV in the pre-edge region between 2,440 and 2,468 (2,100 and 2,140) eV; 0.1 eV between 2,468 and 2,485 (2,140 and 2,160) eV, the main region of interest; and 0.3 eV between 2,485 and 2,520 (2,160 and 2,200) eV with an integration time of 1 s per point. Measurements of the sulfur reference compounds (see Fig. 3) and phosphorus reference compounds (see Fig. 5) were performed with the same step sizes and parameters in transmission mode. The reference compounds (ATP as adenosine-5′-triphosphate-disodium salt hydrate, calcium hydrogen phosphate, silver phosphate, and aqueous phosphoric acid) were purchased from Sigma-Aldrich (St. Louis, MO).

RESULTS AND DISCUSSION

The antibacterial effect of silver ions was determined by conventional plate counting (repeated three times). After 10 min of treatment with silver ions, the count for each type of bacterial cells, *S. aureus*, *E. coli*, and *L. monocytogenes*, was below the detection limit (<1 CFU/ml). In control samples (not treated with silver ions), 10^5 to 10^6 CFU/ml were determined. After treatment of bacterial cells with silver ion solutions, light microscopic investigations showed that some bacterial cells were visibly destroyed or inactivated (*E. coli* was not motile anymore), which agrees with the results of conventional plate counting of treated bacteria and is in accordance with the results reported by Jung et al. (3). The results of the silver *LIII*-edge XANES measurements of silver ion-treated

E. coli, *S. aureus*, and *L. monocytogenes* versus the spectra of silver nitrate solution and silver acetate are shown in Fig. 1. Untreated *S. aureus*, *E. coli*, and *L. monocytogenes* cells were also measured at the Ag *LIII* edge. As expected, no silver was detected (data not shown). The Ag *LIII*-edge XANES spectra of *E. coli* treated with both starting materials, AgNO$_3$ and aqueous Ag [Ag(ac)], are identical. Also, *S. aureus* and *L. monocytogenes* show nearly identical Ag *LIII*-edge XANES spectra after treatment with AgNO$_3$ solution or aqueous Ag(ac) solution, respectively. However, the Ag *LIII*-edge XANES spectra of all three types of bacteria are slightly different from each other and very different from the spectra of AgNO$_3$ and Ag(ac) solutions. Differences in the Ag *LIII*-edge XANES spectra are the prominent peak at 3,352 eV and the shift of the so-called "white line" (22) for silver nitrate (silver acetate) to a higher energy (3,353 eV) for the bacterial samples, indicating a change in the electronic environment. The peak around 3,350 eV is experimentally and theoretically connected to the 2p → 4d transition (22). The intensity at this peak reflects the density of unoccupied states in the Ag 4d band. There is a significant difference in the structure of the bacterial spectra in the range of the shape resonances at about 3,372 eV with the silver nitrate solution and at about 3,380 eV with the silver acetate solution (Fig. 1). The bacterial spectra show an absorption feature (shoulder) at about 3,360 eV that is not present in both solution spectra (Fig. 1). The bacterial samples show significant differences. The intensity of the peak at 3,353 eV is higher for *S. aureus* and *L. monocytogenes* than for *E. coli*, while no energy shift is observed. Further, the intensity of the shoulder at 3,360 eV is higher for *S. aureus* and *L. monocytogenes* than for *E. coli*. These spectral differences point to differences in the chemical environment of the silver ions in the bacteria, which are a first indication of a different biological interaction. In order to understand the character of the bonding of silver in the bacterial environment, organic silver compounds that should be models for the hypothesis described above were measured under the same conditions as those described for the bacterial samples. Inorganic reference compounds (not shown) are not adequate for a fingerprint analysis at the Ag *LIII* edge because the XANES spectra are sensitive beyond the second coordination shell (30). Figure 2 shows Ag *LIII*-edge XANES spectra of the organic silver refer-
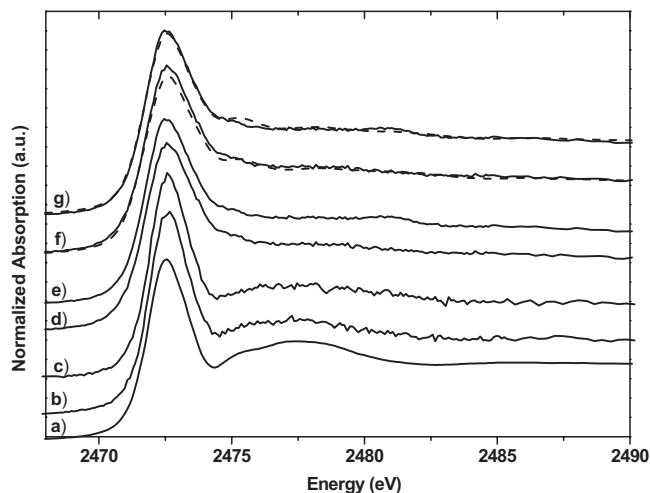
FIG 3 Sulfur *K*-edge XANES spectra of cysteine (a), *E. coli* cells not treated with silver (b), *S. aureus* cells not treated with silver (c), *E. coli* cells treated with silver nitrate (d), and *S. aureus* cells treated with silver nitrate (e); LCF of *E. coli* cells treated with silver nitrate according to Table 2 (broken line) and the experimental results (solid line) (f); and LCF of *S. aureus* cells treated with silver nitrate according to Table 2 (broken line) and the experimental results (solid line) (g). a.u., arbitrary units.

FIG 4 Sulfur *K*-edge XANES spectra of sulfur reference compounds zinc sulfate (a), methionine (b), cysteine (c), glutathione (d), silver-cysteine (e), and silver-glutathione (f). a.u., arbitrary units.

ence compounds together with silver phosphate (to represent ATP) and silver metal. The position of the pre-edge feature at 3,353 eV and a shoulder at 3,360 eV are the main characteristics of silver-histidine. This agrees very well with the bacterial spectra, which is an indication that Ag-N bonding is the dominant interaction. LCF (Table 1 and Fig. 1) was performed with Ag-Cys, Ag-His, Ag-Ala, and Ag–DL-Asp. Represented here is silver bonding to (i) nitrogen (Ag-N) in the form of Ag-histidine, (ii) to sulfur (Ag-S) in the form of Ag-cysteine, and (iii) to oxygen (Ag-O) in the form of Ag–DL-Asp. Ag-alanine represents mixed bonding to both nitrogen and oxygen. For *E. coli*, all four silver-amino acids contribute to the fit with ca. 10 to 40%. For *S. aureus*, on the other hand, silver-histidine and silver-alanine clearly are the dominant contributions (40 to 50%). These fits also show a significant difference in the silver-cysteine contribution between *S. aureus* and *E. coli* (10 versus 24%, respectively). These percentages of silver-cysteine bonds agree with reports on cytoplasmic cysteine levels between 2 and 15% for facultative anaerobic bacteria such as *E. coli* and *S. aureus* (31). Keeping the experiments performed by Kim and coworkers (see introduction above) (5) in mind, additional experiments were performed. Ag ions (from silver nitrate) were added to a mixture of histidine and cysteine solutions (in a 1:1 ratio). Here the ions showed a higher affinity for sulfur than for nitrogen (data not shown) with the formation of Ag-cysteine. In a second experiment, cysteine solution was added to Ag-histidine solution (Ag-His redissolved in water), which again resulted in Ag-cysteine formation. These experiments show clearly that silver bonds first to all of the sulfur available and only then bonds to nitrogen and oxygen.

In order to confirm Ag-S bonding, XANES measurements at the sulfur *K* edge were also carried out. Figure 3 shows the spectra of treated and untreated bacterial samples together with cysteine and the LCF results. Figure 4 shows the set of sulfur reference compounds used for the LCF at the S *K* edge. The S *K*-edge XANES spectra of treated bacteria are different from those of untreated samples. The spectra of the untreated samples of *S. aureus* and *E.*
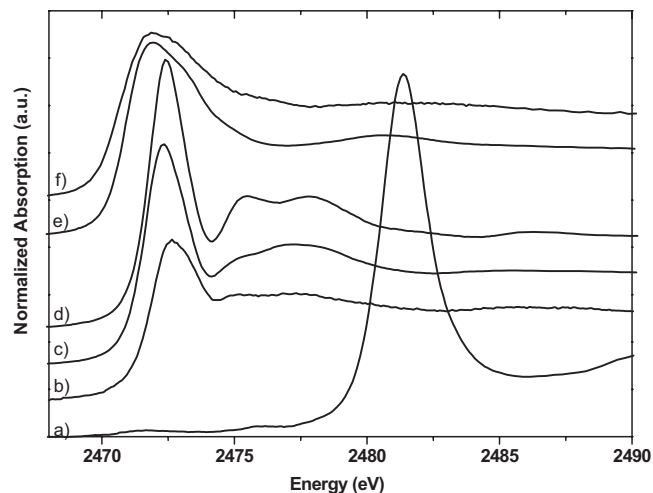
coli are, as expected, very similar to that of cysteine (Fig. 3). They show a white line maximum at 2,472.7 eV and a prominent shape resonance at about 2,477 eV. This shape resonance is absent from the spectra of *S. aureus* and *E. coli* treated with silver ions. The results of the LCF with cysteine, silver-cysteine, glutathione, silver-glutathione, methionine, and zinc sulfate show clearly a dominant contribution of silver-cysteine. This strongly supports the hypothesis of Ag-S bonding.

Bonding of silver to ATP (phosphorus) was examined at the phosphorus *K* edge. Figure 5 shows the P *K*-edge XANES spectra of bacterial cells treated with silver ions and nontreated cells together with reference compounds. The spectral features are identical in the samples with and without the addition of silver ions.
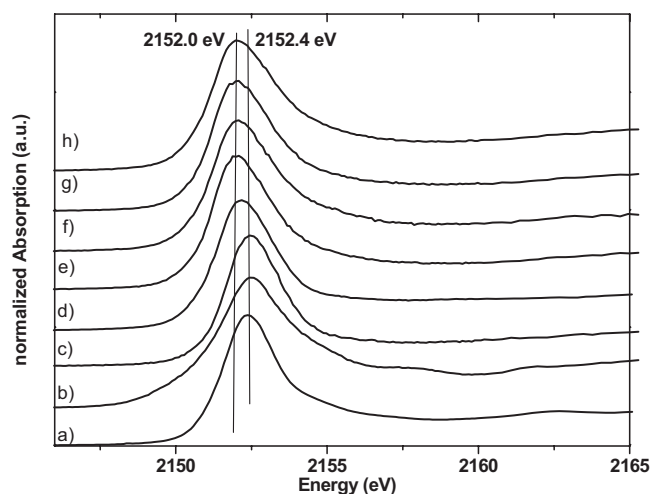

FIG 5 Phosphorus *K*-edge XANES spectra of phosphorus reference compounds and bacterial samples. Shown are results for calcium hydrogen phosphate (a), silver phosphate (b), aqueous phosphoric acid (c), ATP (d), *E. coli* cells not treated with silver (e), *E. coli* cells treated with silver nitrate (f), *S. aureus* not treated with silver (g), and *S. aureus* cells treated with silver nitrate (h). a.u., arbitrary units.

Further, the white line maxima of the spectra of bacterial cells are significantly shifted to a lower energy (2,152.0 eV) than the spectra of the inorganic phosphate compounds (2,152.4 eV). P K-edge XANES spectra are sufficiently sensitive to the chemical environment of P atoms (32). The identical spectral features in the bacterial spectra (Fig. 5) and the significant shift of the white line indicate that silver ions do not interact with or bind to phosphate groups of ATP. Thus, most likely, there is no reaction with phosphate groups of bacterial DNA or any other phosphorus- or phosphate-carrying component.

Conclusions. Using the fingerprint approach for the interpretation of XANES spectra, the present investigation of the antibacterial activity of silver provides some new and very fundamental information about the reaction mechanism. For three types of bacteria that are sensitive to Ag^+ treatment, there are differences in the Ag $LIII$ XANES spectra of silver nitrate and silver acetate solutions from those of bacteria treated with these solutions. This is a clear indication that Ag^+ ions, in fact, do react with bacterial cells and that they do not stay Ag^+ ions in the system. Our experiments with suitable reference compounds show that the preferred binding partner of Ag ions is sulfur, followed by nitrogen and oxygen. The Ag $LIII$-edge spectra of Gram-positive and Gram-negative bacteria treated with either a silver nitrate or a silver acetate solution are different, indicating different interaction mechanisms. The least-squares fitting analysis of the spectra indicates a nondominant Ag-S interaction for all three bacteria, most likely reflecting the fact that S-containing amino acids are not very abundant in living organisms. This observation supports the hypothesis that silver binds strongly to enzymes with sulfur-containing side chains. This bond causes an inhibition of the electron transport chain of the cells (11 and references therein). Ag-N is the dominant binding type in *S. aureus*, and mixed Ag-N and Ag-O binding is dominant in *E. coli*. Both types of bonds seem to be unspecific and might be assigned to bond to the nucleic acids in DNA, resulting in a disturbance of reproduction. On the basis of the XANES investigations at the P K edge, bonding to the phosphate groups in ATP can clearly be ruled out. Thus, our experiments indicate that the antibacterial effect of Ag^+ ions is not due to a specific bond, e.g., Ag-S, but that bonds to various sites (S, N, and O) are likely. Our results also offer a possible explanation for the reported difference in sensitivity to Ag^+ ions between Gram-positive and Gram-negative bacteria. Compared to *E. coli*, *S. aureus* and *L. monocytogenes* have "additional protection," a thick, multilayered peptidoglycan sacculus with a high content of amine and carboxyl groups. The high percentage of Ag-alanine and Ag-histidine that was observed in *S. aureus* and *L. monocytogenes* is notable. One can speculate that a significant portion of the Ag^+ ions binds to the peptidoglycan multilayer in the cell wall or to lipopolysaccharides on the cell wall and that only a smaller portion enters the cell to react with amino acids or DNA.

REFERENCES

1. **Silver S, Phung LT.** 1996. Bacterial heavy metal resistance: new surprises. Annu. Rev. Microbiol. **50:**753–789.
2. **Chopra I.** 2007. The increasing use of silver-based products as antimicrobial agents: a useful development or a cause for concern? J. Antimicrob. Chemother. **59:**587–590.
3. **Jung WK, Koo HC, Kim KW, Shin S, Kim SH, Park YH.** 2008. Antibacterial activity and mechanism of action of the silver ion in *Staphylococcus aureus* and *Escherichia coli*. Appl. Environ. Microbiol. **74:**2171–2178.
4. **Sondi I, Salopek-Sondi B.** 2004. Silver nanoparticles as antimicrobial agent: a case study on *E. coli* as a model for Gram-negative bacteria. J. Colloid Interface Sci. **275:**177–182.
5. **Kim JS, Kuk E, Yu KN, Kim J-H, Park SJ, Lee HJ, Kim SH, Park YK, Park YH, Hwang C-Y, Kim Y-K, Lee Y-S, Jeong DH, Cho M-H.** 2007. Antimicrobial effects of silver nanoparticles. Nanomedicine **3:**95–101.
6. **Li X-Z, Nikaido H, Williams KE.** 1997. Silver-resistant mutants of *Escherichia coli* display active efflux of Ag^+ and are deficient in porins. J. Bacteriol. **179:**6127–6132.
7. **Nies DH.** 2003. Efflux-mediated heavy metal resistance in prokaryotes. FEMS Microbiol. Rev. **27:**313–339.
8. **Yakabe Y, Sano T, Ushio H, Yasunaga T.** 1980. Kinetic studies of the interaction between silver ion and deoxyribonucleic acid. Chem. Lett. **4:**373–376.
9. **Nomiya K, Tsuda K, Sudoh T, Oda M.** 1997. Ag(I)-N bond-containing compound showing wide spectra in effective antimicrobial activities: polymeric silver(I) imidazolate. J. Inorg. Biochem. **68:**39–44.
10. **Davies RL, Etris SF.** 1997. The development and functions of silver in water purification and disease control. Catal. Today **36:**107–114.
11. **Radzig MA, Koksharova OA, Khmel' IA.** 2009. Antibacterial effects of silver ions: effect on growth of Gram-negative bacteria and biofilm formation. Mol. Gen. Mikrobiol. Virusol. **24:**194–199.
12. **Liau SY, Read DC, Pugh WJ, Furr JR, Russell AD.** 1997. Interaction of silver nitrate with readily identifiable groups: relationship to the antibacterial action of silver ions. Lett. Appl. Microbiol. **25:**279–283.
13. **Richards RME, Odelola HA, Anderson B.** 1984. Effect of silver on whole cells and spheroblasts of silver resistant *Pseudomonas aeruginosa*. Microbios **39:**151–158.
14. **Furr JR, Russell AD, Turner TD, Andrews A.** 1994. Antibacterial activity of Actisorb Plus, Actisorb and silver nitrate. J. Hosp. Infect. **27:**201–208.
15. **Bianconi A.** 1988. XANES spectroscopy, p 573–662. *In* Koningsberger DC, Prins RC (ed), X-ray absorption: principles, applications, techniques of EXAFS, SEXAFS and XANES. Wiley, New York, NY.
16. **Rompel A, Cinco RM, Latimer MJ, McDermott AE, Guiles RD, Quintanilha A, Krauss RM, Sauer K, Yachandra VK, Klein MP.** 1998. Sulfur K edge X-ray absorption spectroscopy: a spectroscopic tool to examine the redox state of S-containing metabolites *in vivo*. Proc. Natl. Acad. Sci. U. S. A. **95:**6122–6127.
17. **Prange A, Modrow H.** 2002. X-ray absorption spectroscopy and its application in biological, agricultural and environmental research. Rev. Environ. Sci. Biotechnol. **1:**259–276.
18. **Prange A, Chauvistré R, Modrow H, Hormes J, Trüper HG, Dahl C.** 2002. Quantitative speciation of sulfur in bacterial sulfur globules: X-ray absorption spectroscopy reveals at least three different species of sulfur. Microbiology **148:**267–276.
19. **Lee Y-J, Prange A, Lichtenberg H, Rohde M, Dashti M, Wiegel J.** 2007. In situ speciation of sulfur globules produced from thiosulfate reduction by *Thermoanaerobacter sulfurigignens*. J. Bacteriol. **189:**7525–7529.
20. **Mrse AA, Bryant PL, Hormes FJ, Butler LG, Satyanarayana N, Rambabu B.** 2003. Solid-state NMR and XANES studies of lithium and silver silicate gels synthesized by sol-gel route. J. Non Cryst. Solids **318:**296–304.
21. **Prietzel J, Thieme J, Paterson D.** 2010. Phosphorus speciation of forest-soil organic surface layers using P K edge XANES spectroscopy. J. Plant Nutr. Soil Sci. **173:**805–807.
22. **Behrens P, Aßmann S, Bilow U, Linke C, Jansen M.** 1999. Electronic structure of silver oxides investigated by AgL XANES spectroscopy. Z. Anorg. Allg. Chem. **625:**111–116.

23. **Prange A, Hormes J, Modrow H.** 2008. X-ray absorption spectroscopy as a tool for the detection and identification of sulfur compounds in phototrophic organisms, p 461–482. *In* Hell R, Dahl C, Leustek T, Knaff D (ed), Advances in photosynthesis and respiration, vol 27: sulfur metabolism in phototrophic organisms. Springer, Berlin, Germany.

24. **Hormes J, Scott JD, Suller V.** 2006. Facility update: the Center for Advanced Microstructures and Devices: a status report. Synchrotron Radiat. News **19:**27–30.

25. **Nomiya K, Takahashi S, Noguchi R, Nemoto S, Takayama T, Oda M.** 2000. Synthesis and characterization of water-soluble silver(I) complexes with L-histidine (H$_2$his) and (S)-(−)-2-pyrrolidone-5-carboxylic acid (H$_2$pyrrld) showing a wide spectrum of effective antibacterial and antifungal activities. Crystal structures of chiral helical polymers [Ag(Hhis)]$_n$ and {[Ag(Hpyrrld)]$_2$}$_n$ in the solid state. Inorg. Chem. **39:**3301–3311.

26. **Nomiya K, Yokoyama H.** 2002. Syntheses, crystal structures and antimicrobial activities of polymeric silver(I) complexes with three amino-acids [aspartic acid (H$_2$asp), glycine (Hgly) and asparagine (Hasn)] J. Chem. Soc. Dalton Trans. **12:**2483.

27. **Pakhomov PM, Ovchinnikov MM, Khizhnyak SD, Lavrienko MV, Nierling W, Lechner MD.** 2004. Study of gelation in aqueous solutions of cysteine and silver nitrate. Colloid J. **66:**65–70.

28. **Demaret A, Abraham F.** 1987. Structure du L-α-alaninate d'argent. Acta Crystallogr. C **43:**1519–1521.

29. **Ravel B, Newville M.** 2005. ATHENA, ARTEMIS, HEPHAESTUS: data analysis for X-ray absorption spectroscopy using IFEFFIT. J. Synchrotron Radiat. **12:**537–541.

30. **Bovenkamp GL.** 2013. X-ray absorption spectroscopy in biological systems: opportunities and limitations. Ph.D. dissertation. University of Bonn, Bonn, Germany.

31. **Daniels R, Mellroth P, Bernsel A, Neiers F, Normark S, von Heijne G, Henriques-Normark B.** 2010. Disulfide bond formation and cysteine exclusion in Gram-positive bacteria. J. Biol. Chem. **285:**3300–3309.

32. **Rouff AA, Rabe S, Nachtegaal M, Vogel F.** 2009. X-ray absorption fine structure study of the effect of protonation on disorder and multiple scattering in phosphate solution and solids. J. Phys. Chem. A **113:**6895–6903.